Contract No.:

This manuscript has been authored by Savannah River Nuclear Solutions (SRNS), LLC under Contract No. DE-AC09-08SR22470 with the U.S. Department of Energy (DOE) Office of Environmental Management (EM).

Analysis of Venting of a Resin Slurry

James E. Laurinat[1]
Savannah River National Laboratory
Savannah River Site
Aiken, South Carolina 29808
email: james.laurinat@srnl.doe.gov

Steve J. Hensel
Fellow ASME
Savannah River Nuclear Solutions LLC
Savannah River Site
Aiken, South Carolina 29808
email: steve.hensel@srnl.doe.gov

ABSTRACT

A resin slurry venting analysis was conducted to address safety issues associated with over-pressurization of ion exchange columns used in the plutonium uranium redox extraction (PUREX) process at the U. S. Department of Energy's (DOE's) Savannah River Site (SRS). If flow to these columns were inadvertently interrupted, an exothermic runaway reaction could occur between the ion exchange resin and the nitric acid used in the feed stream. The nitric acid-resin reaction generates significant quantities of noncondensable gases, which would pressurize the column. To prevent the column from rupturing during such events, rupture disks are installed on the column vent lines. The venting analysis models accelerating rate calorimeter (ARC) tests and data from tests that were performed in a vented test vessel with a rupture disk. The tests showed that the pressure inside the test vessel continued to increase after the rupture disk opened, though at a slower rate than prior to the rupture. The increase in the vessel pressure is modeled as a transient phenomenon associated with expansion of the resin slurry/gas mixture upon rupture of the disk. It is postulated that the maximum pressure at the end of this expansion is limited by energy minimization to approximately 1.5 times the rupture disk burst pressure. The magnitude of this pressure increase is consistent with the measured pressure transients. The results of this analysis demonstrate the need to allow for a margin between the design pressure and the rupture disk burst pressure in similar applications.

INTRODUCTION

This document presents an analysis of vent flow rates and pressure transients during a postulated reaction excursion in one of the Savannah River Site (SRS) plutonium uranium redox extraction (PUREX) process anion exchange columns. The anion

[1] Corresponding author

exchange columns remove plutonium from nitric acid solutions by adsorbing plutonium nitrate on a styrene-based resin. If flow to one of these columns were interrupted, the column temperature would rise due to heating by radiolysis, the adsorption reaction, and an acid-resin decomposition reaction. This heat would selectively drive off water from the acid solution, eventually leaving an azeotropic acid solution with an atmospheric boiling point of about 394 K (121 °C). Additional heating would then result in a rapid and uncontrolled pressure rise due to boiling of the nitric acid and generation of vapor from the oxidation of the resin. The result would be either a column fire or, more likely, rupture of the column due to overpressure. The goal of this study is to determine if the column vent lines are sufficiently large to relieve the pressure in the column to prevent a rupture.

The analyses in this report use pressure transients based on a series of vent tests and ARC measurements conducted in 1986. These transients are combined with a homogeneous two-phase (gas-slurry) model of flow through the vent lines. The two-phase flow model is benchmarked with steam-water choked flow measurements.

DESCRIPTION OF VENT TESTS

In 1986, the DuPont Engineering Test Center conducted two series of tests to size a relief vent for the SRS PUREX process anion exchange columns in the event of a runaway resin-acid reaction. The first series used an ARC to characterize the nitric acid-resin reaction. The second series used a small vented pressure vessel to simulate the reaction in a column. Both series of tests used a mixture of 8000 mol/m^3 (8 M) nitric acid and Dowex 21K resin loaded with thorium, a plutonium surrogate. The resin was irradiated to simulate the degradation that would occur in an actual column.

The ARC tests used a sample consisting of 0.00121 kg of resin and 0.00128 kg of 8000 mol/m^3 nitric acid, of which 0.00068 kg was molecular HNO_3. Table 1 summarizes the reaction data obtained from these tests.

The reaction rate constant also was measured. However, because the rate was measured at a low temperature, the rate for the simulations was derived from the pressure vessel data.

The pressure vessel tests used a cylindrical can with an internal volume of about 0.0001 m^3. The vessel had a small top vent with a cross-sectional flow area scaled down so that the flow area to volume ratio was the same as that of the existing vent in the anion exchange column. For several tests, there was also a bottom vent with a rupture disk downstream to simulate pressure relief. The first series of pressure vessel tests used the same resin-acid mix as the ARC tests. A second series of tests used Dowex MSA-1 resin. Figure 1 depicts the pressure vessel setup for these tests.

Transient data were provided for four tests, two of which, designated as Tests 14, and 15, are analyzed in this study. Tests 14 and 15 used a 0.057-kg sample of wet, drained resin with 0.0126 kg of acid and had a 0.0112-m (0.44-in.) diameter bottom vent protected by rupture disks. The rupture disk burst pressures were 1.58E6 Pa (215 psig) for Test 14 and 5.22E5 Pa (61 psig) for Test 15. Tables 2 and 3 list the transient pressures for these tests.

The rate constant *G* for the rate of pressure increase is evaluated using data from resin vent test 14 taken prior to disk rupture. During this initial phase of the transient, it is assumed that no venting occurs and that the vapor volume fraction remains constant. Because the rate constant *G* is measured just prior to disk rupture, the initial conditions are defined as occurring at any time before venting begins. With these restrictions, the rate constant is given by

$$G = \left(\frac{d\, ln\left(\frac{P}{P_0} \right)}{dt} \right)_{nv} \tag{1}$$

where the subscript *nv* denotes no venting. To calculate *G*, a least squares regression analysis was performed (see Fig. 2). The calculated value for *G* is 71.3 1/s.

DESCRIPTION OF VENTING MODEL

The model for the pressure transient in the ion exchange columns and the flow out the vent pipes combines a vapor generation rate expression with a criterion for choked flow in the vents. The vapor generation rate expression is based on the results of the pressure vessel tests described in the Description of Vent Tests section. The choked flow criterion is derived from a homogeneous flow model in which the vapor and the slurry are assumed to flow through the vent at the same velocity. Vapor and slurry mass flow rates are assumed to be proportional to the amount of each phase remaining in the column, i.e., the column is assumed to be uniform. Two-phase mixture composition and temperature changes in the vents are ignored because the pressure and temperature changes are small during the short transit time through the vent.

The choked flow criterion is applied to calculate the vent velocity. This criterion is derived by combining the integral Bernoulli equation with a constant flow area momentum balance. The derivation assumes that both slurry and vapor phases flow at the same velocity and that the temperature is nearly constant during the transit through the vent. The derivation is a two-phase extension of the isothermal choked flow analysis presented by Lapple [1] and others.

Moody [2] derived a model that accounts for slip. Although his model more accurately predicts choked flow rates at lower pressures, it is not used in this study. One reason it is not used is that it is not apparent that slip would occur to as great an extent in a slurry as in pure liquid-vapor systems, due to the high slurry-phase viscosity.

Due to a lack of data for slurry-vapor mixtures, the choking criterion is evaluated by comparing it with steam-water data. Comparisons are made with measurements of vent exit flow rates at different exit and stagnation pressures. The exit pressure data serve as a direct benchmark of the choking criterion, and the stagnation pressure data serve as a test of the combination of the choking criterion and the homogeneous flow models.

Two different choked flow models were examined, a so-called frozen flow model that neglects flashing of volatile liquid during flow through the vent and an equilibrium flow model that includes flashing. Figures 3 and 4 compare choking predictions from the frozen and thermal equilibrium flow models with measured choking rates at different stagnation pressures and qualities [3]. These figures show that the frozen flow model is more accurate and therefore more appropriate than the thermal equilibrium model.

Henry and Fauske [4] suggested the use of the single-phase discharge coefficient of 0.84 for venting from an orifice. Predictions of choked flow rates using the frozen flow model with this discharge coefficient also appear in Figs. 3 and 4. Use of the discharge coefficient improves agreement between predicted and measured choking rates, but only slightly. In this analysis, the discharge coefficient is set equal to one.

To calculate the rate of pressure change during venting, the frozen flow model is combined with vapor phase and slurry phase mass balances. The pressure is introduced through the vapor phase mass balance by stipulating that the temperature remain constant during venting, so that the vapor density is proportional to the pressure. This approximation should not introduce significant errors, because pressure changes due to volumetric expansion should be smaller than pressure changes due to venting and to gas formation by reaction. For brevity's sake, this manuscript does not present details of the venting calculations.

MODELING OF THE EFFECT OF A RUNAWAY REACTION ON VENTING

The no-slip, frozen flow venting model just described does not account for the effect of a concurrent runaway reaction. To model the initial slurry expansion, a two-dimensional axisymmetric analysis is required. The axisymmetric vapor and slurry phase mass balances are, respectively,

$$\frac{\partial \varepsilon \rho_g}{\partial t} + \frac{\partial \varepsilon \rho_g v_z}{\partial z} + \frac{1}{r}\frac{\partial r \varepsilon \rho_g v_r}{\partial r} = \varepsilon_0 \rho_g \frac{1-\varepsilon}{1-\varepsilon_0} G \tag{2}$$

and

$$\rho_s \frac{\partial (1-\varepsilon)}{\partial t} + \rho_s \frac{\partial (1-\varepsilon) v_z}{\partial z} + \frac{\rho_s}{r}\frac{\partial r (1-\varepsilon) v_r}{\partial r} = 0 \tag{3}$$

The rate constant on the right side of Eq. (2) is multiplied by $(1-\varepsilon)/(1-\varepsilon_0)$ to account for the decrease in the slurry bulk density as the slurry mixture expands. The factor $\varepsilon_0 \rho_g$ is included to normalize the rate constant *G*.

The mass balances are combined with the ideal gas law for the vapor,

$$\rho_g = \frac{M_g P}{R_g T} \tag{4}$$

to get the following expressions for the rates of change of the pressure and the vapor volume fraction in terms of the substantial derivative (D/Dt),

$$\frac{DP}{Dt} = -\frac{P}{\varepsilon}\left(\frac{\partial v_z}{\partial z} + \frac{1}{r}\frac{\partial r v_r}{\partial r}\right) + \frac{\varepsilon_0 (1-\varepsilon)}{\varepsilon (1-\varepsilon_0)} G P \tag{5}$$

and

$$\frac{D\varepsilon}{Dt}=\left(1-\varepsilon\right)\left(\frac{\partial v_z}{\partial z}+\frac{1}{r}\frac{\partial r v_r}{\partial r}\right) \tag{6}$$

The axial and radial momentum balances, in terms of the substantial derivative, are

$$\frac{Dv_z}{Dt}=-\frac{1}{\varepsilon\rho_g+\left(1-\varepsilon\right)\rho_s}\frac{\partial P}{\partial z} \tag{7}$$

and

$$\frac{Dv_r}{Dt}=-\frac{1}{\varepsilon\rho_g+\left(1-\varepsilon\right)\rho_s}\frac{\partial P}{\partial r} \tag{8}$$

Elimination of the velocity gradient terms from Eqs. (5) and (6) gives

$$\frac{DP}{Dt}+\frac{P}{\varepsilon\left(1-\varepsilon\right)}\frac{D\varepsilon}{Dt}=\frac{\varepsilon_0\left(1-\varepsilon\right)}{\varepsilon\left(1-\varepsilon_0\right)}GP \tag{9}$$

or

$$\frac{D}{Dt}\left(\frac{\varepsilon P}{1-\varepsilon}\right)=\frac{\varepsilon_0}{1-\varepsilon_0}GP \tag{10}$$

Another equation is needed to solve for ε and P. This is obtained by recasting Eq. (5) as an ordinary, second-order differential equation in time, i.e., a dispersion equation, in which the first two terms account for dispersion of pressure and the last term represents a pressure source. This is accomplished by taking the substantial derivative, which gives

$$\frac{D^2P}{Dt^2}=-\frac{D}{Dt}\left(\frac{P}{\varepsilon}\left(\frac{\partial v_z}{\partial z}+\frac{1}{r}\frac{\partial r v_r}{\partial r}\right)\right)+\frac{D}{Dt}\left(\frac{\varepsilon_0\left(1-\varepsilon\right)}{\varepsilon\left(1-\varepsilon_0\right)}GP\right) \tag{11}$$

It is assumed that the first two terms in this equation both account for pressure dispersion, so they should be proportional to each other. Therefore,

$$\frac{D^2P}{Dt^2}+\frac{D}{Dt}\left(\frac{P}{\varepsilon}\left(\frac{\partial v_z}{\partial z}+\frac{1}{r}\frac{\partial r v_r}{\partial r}\right)\right)=\beta\frac{D^2P}{Dt^2} \tag{12}$$

where β is a proportionality constant relating the substantial derivative and the divergence of the pressure (the first and second terms in Eq. (5)). β is assumed to be positive.

The source term (the last term in Eq. (5)) can be expressed as the product of a growth rate constant *G* that is invariant and the substantial derivative of the pressure. The rate of pressure increase due to reaction is exponential, so the substantial derivative, and therefore the entire term, scales proportionally with the pressure. In other words,

$$\frac{D}{Dt}\left(\frac{\varepsilon_0\left(1-\varepsilon\right)}{\varepsilon\left(1-\varepsilon_0\right)}GP\right)=\alpha^2P \tag{13}$$

where α represents a wave number.

The two preceding assumptions combine to give

$$\beta \frac{D^2 P}{Dt^2} - \alpha^2 P = 0 \tag{14}$$

There are three possible types of solutions to this equation, simultaneous exponentially growing solution and decaying solutions corresponding to positive and negative square roots of α^2 and a linear solution given by $\alpha = 0$. The growing solution is ruled out by the assumption that the pressure field is dispersive. A negative α of any significant magnitude will generate a solution that quickly diminishes. That leaves the linear solution, which requires that

$$\frac{D^2 P}{Dt^2} = 0 \tag{15}$$

and

$$\frac{D}{Dt}\left(\frac{\varepsilon_0 (1-\varepsilon)}{\varepsilon (1-\varepsilon_0)} GP \right) = 0 \tag{16}$$

The following analysis will demonstrate that these requirements are consistent with each other.

Differentiation of Eq. (16) yields

$$\frac{\varepsilon_0 (1-\varepsilon)}{\varepsilon (1-\varepsilon_0)} G \frac{DP}{Dt} - \frac{\varepsilon_0}{\varepsilon^2 (1-\varepsilon_0)} GP \frac{D\varepsilon}{Dt} = 0 \tag{17}$$

This expression can be combined with Eq. (9) to get

$$\frac{DP}{Dt} = \frac{1}{2} \frac{\varepsilon_0 (1-\varepsilon)}{\varepsilon (1-\varepsilon_0)} GP \tag{18}$$

Substitution of this equation into Eq. (9) gives an ordinary equation for the vapor volume fraction.

$$\frac{D\varepsilon}{Dt} = \frac{1}{2} \frac{\varepsilon_0 (1-\varepsilon)^2}{1-\varepsilon_0} G \tag{19}$$

Equations (18) and (19) are ordinary differential equations, so they may be integrated with respect to time, if one assumes that the pressure inside the slurry is independent of position. With the initial conditions, when $t = 0$,

$$\varepsilon = \varepsilon_0 \tag{20}$$

and

$$P = P_0 \tag{21}$$

Integration of Eq. 19 gives

$$\varepsilon = \frac{\varepsilon_0 \left(1 + \frac{1}{2} Gt \right)}{1 + \frac{1}{2} Gt \varepsilon_0} \tag{22}$$

Substitution of this solution in Eq. (19) and integration give the solution for the pressure.

$$P = P_0\left(1+\frac{1}{2}Gt\right) \tag{23}$$

It may be noted that this is a linear solution, as stipulated by Eq. (15).

A solution for the stagnation pressure can be obtained by comparing this solution to Eq. (5), with the velocity components set at zero. This results in the following expression:

$$\frac{dP_s}{dt} = \frac{\varepsilon_0\left(1-\varepsilon_s\right)}{\varepsilon_s\left(1-\varepsilon_0\right)}GP_s \tag{24}$$

Because the mass balances ignore the volume of slurry lost to evaporation, the stagnation vapor volume fraction remains constant. Thus,

$$\varepsilon_s = \varepsilon_0 \tag{25}$$

A comparison of Eqs. (19) and (24) shows that when $t = 0$,

$$\frac{d\,ln\left(P_s\right)}{dt} = 2\frac{D\,ln\left(P\right)}{Dt} \tag{26}$$

It follows from this expression and Eq. (23) that

$$P_s = P_0\left(1+\frac{1}{2}Gt\right)^2 \tag{27}$$

The intrinsic transients predicted by Eqs. (22) and (23) will continue only so long as the expansion of the slurry results in a net decrease in the energy of the slurry per unit mass. Over a given time interval, this change in the energy of the slurry due to its expansion is just the difference between the change in the actual dynamic head for the expanding slurry and the static head for a stationary slurry, divided by the slurry density. Accordingly, for a time interval Δt, the change in the slurry energy per unit mass due to expansion, *I*, is given by

$$I = \frac{1}{\rho}\left(\frac{D}{Dt}\left(P+\frac{1}{2}\rho v^2\right)-\frac{\partial P}{\partial t}\right)\Delta t \tag{28}$$

where the partial derivative of the pressure denotes the time rate of change for the static head and the substantive derivative is the rate of change for the dynamic pressure.

A comparison of Eqs. (18) and (24) shows that the static pressure increases twice as fast for a stationary slurry as for an expanding slurry. Therefore,

$$\frac{\partial P}{\partial t} = 2\frac{DP}{Dt} \tag{29}$$

The density in Eq. (28) is the slurry mixture density, defined as

$$\rho = \frac{\varepsilon_s\rho_{gs}+\left(1-\varepsilon_s\right)\rho_s}{1-\varepsilon_s+\frac{P_s}{P}\varepsilon_s} \tag{30}$$

The density appears outside the time derivative because the differences in the rates of increase of the dynamic and static heads apply to the same slurry.

The velocity is calculated by applying a pseudo-steady state approximation that the acceleration of the slurry from its stagnation state occurs over a much shorter time

scale than increases in pressure due to the decomposition reaction. With this approximation, the slurry velocity can be calculated from the integral momentum balance. The generalized form of this momentum balance is

$$-\int_{P_s}^{P}\left(\frac{1}{\rho}\right)dP=\frac{v^2}{2} \tag{31}$$

Substitution of the density from Eq. (30) and integration give

$$\frac{1}{2}v^2=\frac{\varepsilon_s P_s\, ln\left(\frac{P_s}{P}\right)+\left(1-\varepsilon_s\right)\left(P_s-P\right)}{\varepsilon_s\rho_{gs}+\left(1-\varepsilon_s\right)\rho_s} \tag{32}$$

The desired expression for *I* is obtained by substituting for the density from Eq. (30), the velocity from Eq. (32), and the time derivative of the pressure from Eq. (29). This yields

$$I=\frac{1-\varepsilon_s+\varepsilon_s\frac{P_s}{P}}{\varepsilon_s\rho_{gs}+\left(1-\varepsilon_s\right)\rho_s}\left(\frac{D}{Dt}\left(\frac{P_s+\varepsilon_s P_s\, ln\left(\frac{P_s}{P}\right)}{1-\varepsilon_s+\varepsilon_s\frac{P_s}{P}}\right)-2\frac{DP}{Dt}\right)\Delta t \tag{33}$$

The value of *I* reaches a minimum as the pressure drops. At this minimum, the expansion ceases, since any further decrease in the pressure would increase the dynamic energy of the slurry. Thus, the minimum slurry pressure is determined by the condition

$$\frac{\partial I}{\partial P}=0 \tag{34}$$

Equations (33) and (34) may be solved by using a Newton iteration. Let

$$y\equiv\frac{P_s}{P} \tag{35}$$

In terms of *y*, the solution for *I* becomes

$$I=\left(\begin{array}{l}\frac{\left(\varepsilon_s-\varepsilon_s^2\right)\left(y^2-y\right)}{\left(1-\varepsilon_s+\varepsilon_s y\right)}\\ +\frac{\varepsilon_s^2 y^2\, ln\left(y\right)}{\left(1-\varepsilon_s+\varepsilon_s y\right)}\\ -2\left(1-\varepsilon_s+\varepsilon_s y\right)\end{array}\right)\frac{1}{\varepsilon_s\rho_{gs}+\left(1-\varepsilon_s\right)\rho_s}\frac{DP}{Dt}\Delta t \tag{36}$$

with

$$\frac{dI}{dy}=0 \tag{37}$$

Equation (36) is a transcendental equation, so the solution to Eqs. (36) and (37) must be recursive. The following Newton iteration is used to obtain a converging recursive solution.

$$y = y - \frac{\frac{dI}{dy}}{\frac{d^2 I}{dy^2}} \tag{38}$$

The solution in terms of pressures is given by

$$\frac{P_s}{P} = \frac{\left(\begin{array}{l} 3 - 6\varepsilon_s + 3\varepsilon_s^2 + \left(2\varepsilon_s - 2\varepsilon_s^2\right)\frac{P_s}{P} \\ + \left(\varepsilon_s - \varepsilon_s^2\right)\frac{P_s^2}{P^2} + \varepsilon_s^2 \frac{P_s^2}{P^2} ln\left(\frac{P_s}{P}\right) \end{array} \right)}{\left(\begin{array}{l} 2 - 5\varepsilon_s + 3\varepsilon_s^2 + \left(2\varepsilon_s - 3\varepsilon_s^2\right)\frac{P_s}{P} \\ + \left(2\varepsilon_s - 2\varepsilon_s^2 + 2\varepsilon_s^2 \frac{P_s}{P} \right) ln\left(\frac{P_s}{P}\right) \end{array} \right)} \tag{39}$$

This solution relates the minimum actual pressure to the stagnation pressure. The desired solution is a relation between this pressure and the pressure at the start of the transient. From Eqs. (23) and (27), it is apparent that

$$\frac{P}{P_0} = \frac{P_s}{P} \tag{40}$$

Equations (25), (39), and (40) combine to yield the recursive relation

$$\frac{P}{P_0} = \frac{\left(\begin{array}{l} 3 - 6\varepsilon_0 + 3\varepsilon_0^2 + \left(2\varepsilon_0 - 2\varepsilon_0^2\right)\frac{P}{P_0} \\ + \left(\varepsilon_0 - \varepsilon_0^2\right)\frac{P^2}{P_0^2} + \varepsilon_0^2 \frac{P^2}{P_0^2} ln\left(\frac{P}{P_0}\right) \end{array} \right)}{\left(\begin{array}{l} 2 - 5\varepsilon_0 + 3\varepsilon_0^2 + \left(2\varepsilon_0 - 3\varepsilon_0^2\right)\frac{P}{P_0} \\ + \left(2\varepsilon_0 - 2\varepsilon_0^2 + 2\varepsilon_0^2 \frac{P}{P_0} \right) ln\left(\frac{P}{P_0}\right) \end{array} \right)} \tag{41}$$

According to the preceding analysis, after the rupture disk bursts, the slurry undergoes an initial period of expansion during which the actual and stagnation pressures increase as specified by Eqs. (23) and (27). This initial expansion ceases when the actual pressure reaches the value defined by Eq. (41). Subsequently, the rates of expansion and pressure change are governed by the vent flow rate calculated from the no-slip, frozen flow venting model.

The minimum ratio for the pressure increase after the rupture disk bursts is 1.5, if the vapor volume fraction approaches zero. At high vapor volume fractions, the vapor flow will disengage from the slurry flow, and the rate of venting will increase to the level predicted by the frozen flow venting model. As the resin-acid reaction proceeds, the vapor volume fraction should rise, and the pressure should increase as predicted by Eq. (41), until disengagement occurs.

Information on vapor volume fractions for venting of slurries is lacking; the only way to estimate the limiting vapor volume fraction for disengagement is by analogies to gas-liquid flows and flows in gas-sparged fluidized beds containing slurries. For bubbly gas-liquid flow, the limiting vapor volume fraction for disengagement is approximately 0.25 [3]. For gas-liquid-solid fluidized beds, the presence of a significant fraction of solids in the slurry reduces the gas phase hold-up. Generally, the gas volume fraction decreases as the sparging rate increases. One test measured a constant gas volume fraction of 0.19, based on bed expansion, over a range of higher sparging rates [5, Fig. 5]. This may indicate that a limiting condition for complete fluidization of the bed was reached. Based on these observations, the limiting vapor volume fraction at vapor disengagement is approximately 0.20.

Using results from the preceding analyses, the rate constant *G* given by Eq. 1 also can be evaluated from the data taken after disk rupture. During venting, the rate constant is given by

$$G = \frac{2}{P_0}\left(\frac{dP}{dt}\right)_v \tag{42}$$

where the subscript v denotes venting. To calculate G, linear least square regression analyses were performed using data from Tests 14 and 15 (see Fig. 5). The regression of the Test 14 data gives a value for *G* of 63.6 1/s, and the regression of the Test 15 data gives 64.1 1/s. These values are in approximate agreement with the estimate of 71.3 1/s, obtained from the regression of the data prior to venting. Much of the difference between the rates before and after venting might be due to uncertainties in the starting time for the reaction excursion, which would affect the calculations prior to venting. The value of 64.1 1/s from the regression of the Test 15 data is the best estimate of the true rate and is therefore used in simulations of the venting pressure transients.

RESULTS AND DISCUSSION

The results for Tests 14 and 15 are compared with computer simulations of venting pressure transients. In the computer simulation, the mass balance for the test chamber is integrated with respect to time, with the frozen flow, no-slip choking criterion applied at each time step. Two sets of calculations were performed, one that neglects the effect of the runaway reaction on the initial rate of expansion following the rupture disk burst and a second that includes this effect. The computer model considers only flow out the bottom vent. Slurry expansion inside the test apparatus and venting of vapor out the top vent are neglected.

Figure 6 compares the model calculations with the test measurements for venting without any allowance for the effect of the resin reaction. Since the initial vapor volume fraction was not known, calculations were performed for a series of four initial values for this parameter: ε_0 = 0.05, 0.10, 0.15, and 0.20; results for all four vapor volume fractions are shown. (The initial time for the disk rupture was estimated by interpolating the test data, so the initial data point does not represent an actual measurement.) As Fig. 6 shows, the model predicts that the bottom orifice was sufficiently large to vent both tests. However, the model fails to account for the observed initial increase in the pressure subsequent to the rupture disk burst.

Figure 7 compares model calculations with test results when the effect of the runaway reaction is incorporated. Again, calculations were performed for ε_0 = 0.05, 0.10, 0.15, and 0.20. With the addition of the runaway reaction effect, the predictions of the model agree closely with the test data during the measurement period with respect to the magnitude of the pressure increase following the rupture disk burst. At later times, the model predicts that the pressure should decrease relatively rapidly to atmospheric pressure as the test chamber vents.

The model predicts that the vessel pressure should decrease more rapidly to ambient conditions for test 14, which implies that the vessel should vent its contents sooner than for test 15. The model demonstrates that changes in the assumed initial vapor volume fraction primarily affect the magnitude of the pressure overshoot shown by Fig. 7; the amount of overshoot increases as the assumed initial vapor volume fraction increases. The results in Figs. 6 and 7 indicate that, once free venting begins, the venting rate is insensitive to the assumed initial vapor volume fraction.

SUMMARY AND CONCLUSION

In 1986, resin venting tests were conducted to address safety issues for operation of the PUREX process anion exchange columns at SRS. The tests measured the ability of a rupture disk to protect a column from over-pressurization due to the generation of noncondensable gases by a runaway resin/nitric acid reaction. The test results showed that the test vessel pressure continued to increase after the disks ruptures.

This report presents an analysis that demonstrates that this pressure overshoot is a transient phenomenon associated with simultaneous pressurization and venting. The analysis predicts that the rate of pressure increase after venting is half the rate of increase prior to venting. The analysis also predicts that, for a rapidly expanding flow, the pressure should increase to a minimum of 1.5 times the pressure at the time of rupture; the pressure overshoot increases as the initial vapor volume fraction increases. Results for the two tests that were analyzed are in good agreement with this prediction. Measured pressures increased to 1.50 times the pressure at the time of rupture for test 14 and to 1.59 times the pressure at the time of rupture for test 15. For both tests, venting analysis showed that the rupture disk should have been able to relieve the vessel pressure in the absence of these transient effects. The venting calculations assumed choked two-phase flow with no slip velocity and no gas generation during flow through the vent.

This study demonstrates the need to account for transient pressure overshoot when designing pressure relief systems for similar applications.

ACKNOWLEDGMENT

J. E. Johnston of DuPont's Engineering Test Center is acknowledged for his efforts in designing and performing the resin venting tests and obtaining the data used in this analysis.

FUNDING DATA

This manuscript has been authored by Savannah River Nuclear Solutions, LLC under Contract No. DE-AC09-08SR22470 with the U.S. Department of Energy.

NOMENCLATURE

G	reaction rate constant, 1/s
I	change in the slurry energy per unit mass due to expansion, defined by Eq. (33), J/kg
M_g	molecular weight of the gas, kg/mol
P	pressure in vessel, Pa
P_s	stagnation pressure, Pa
P_0	initial pressure in vessel, or pressure at the time of disk rupture, Pa
r	radial distance from the centerline of the test chamber, m
R_g	gas constant, J/(mol K)
t	time after start of reaction excursion, s
T	absolute temperature, K
v	velocity at the vent or in the vent pipe, m/s
v_r	radial velocity, m/s
v_s	vent velocity at stagnation conditions, m/s
v_z	axial velocity, m/s
y	ratio of stagnation pressure to pressure at vent entrance or to pressure in test chamber
z	streamwise distance from the entrance of the vent pipe or axial distance from the bottom of the test chamber, m

α	wave number for dispersion equation (see Eqs. (13) and (14)), 1/s
β	proportionality constant relating the substantial derivative and the divergence of the pressure (the first and second terms in Eq. (12))
ε	vapor volume fraction
ε_s	vapor volume fraction at stagnation conditions
ε_0	initial vapor volume fraction
ρ	slurry mixture density, kg/m^3
ρ_g	vapor density, kg/m^3
ρ_{gs}	vapor density at stagnation conditions, kg/m^3
ρ_s	slurry density, kg/m^3

REFERENCES

[1] Lapple, C. E., 1943, "Isothermal and Adiabatic Flow of Compressible Fluids, " Trans. Am. Inst. Chem. Eng., **39**(4), pp. 385-432.

[2] Moody, F. J., 1965, "Maximum Flow Rate of a Single Component, Two-Phase Mixture," ASME J. Heat Trans., **87**(1), pp. 134-142.

[3] Hsu, Y.-Y., and Graham, R. W., 1986, *Transport Processes in Boiling and Two-Phase Systems, Including Near Critical Fluids*, American Nuclear Society, La Grange Park, IL.

[4] Henry, R. E., and Fauske, H. K., 1971, "The Two-Phase Critical Flow of One-Component Mixtures in Nozzles, Orifices, and Short Tubes," ASME J. Heat Trans., **93**(2), pp. 179-187.

[5] Mena, P. C., Ruzicka, M. C., Rocha, F. A., Teixeira, J. A., and Drahoš, J., 2005, "Effect of Solids on Homogeneous-Heterogeneous Flow Regime Transition in Bubble Columns, " Chem. Eng. Sci., **60**(22), pp. 6013-6026.

Table 1. Results of ARC tests

Heat of reaction	6.19E5 J/kg total mixture
Gas evolution	3.67 mol/kg total mixture
Activation energy	1.06E5 J/mol

Table 2. Transient pressures for resin vent test 14

Time	Vessel Pressure
0.041 s	4.46E5 Pa (50 psig)
0.046 s	6.18E5 Pa (75 psig)
0.050 s	7.91E5 Pa (100 psig)
0.056 s	1.308E6 Pa (175 psig)
0.061 s	1.825E6 Pa (250 psig)
0.066 s	1.915E6 Pa (263 psig)
0.072 s	2.370E6 Pa (329 psig)[a]

[a] maximum measured pressure

Table 3. Transient pressures for resin vent test 15

Time	Vessel Pressure
0.031 s	3.63E5 Pa (38 psig)
0.043 s	4.46E5 Pa (50 psig)
0.048 s	5.36E5 Pa (63 psig)
0.051 s	6.18E5 Pa (75 psig)
0.058 s	7.08E5 Pa (88 psig)
0.060 s	7.22E5 Pa (90 psig)
0.061 s	7.91E5 Pa (100 psig)
0.065 s	8.32E5 Pa (106 psig)[a]

[a] maximum measured pressure

Fig. 1. Cross-section of test apparatus

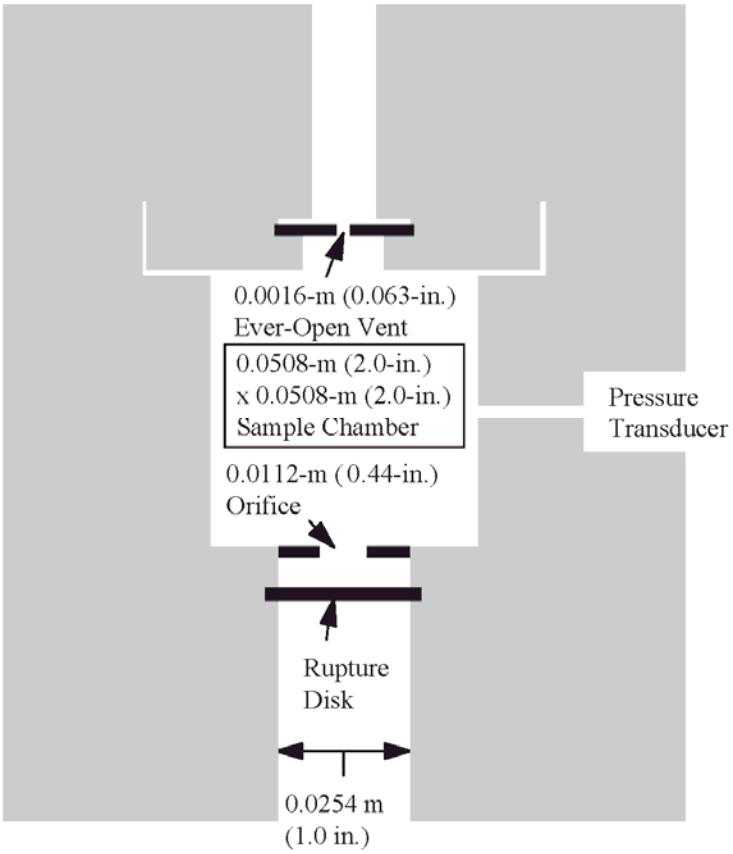

Fig. 2. Correlation of pressure transient for resin vent test 14 prior to disk rupture

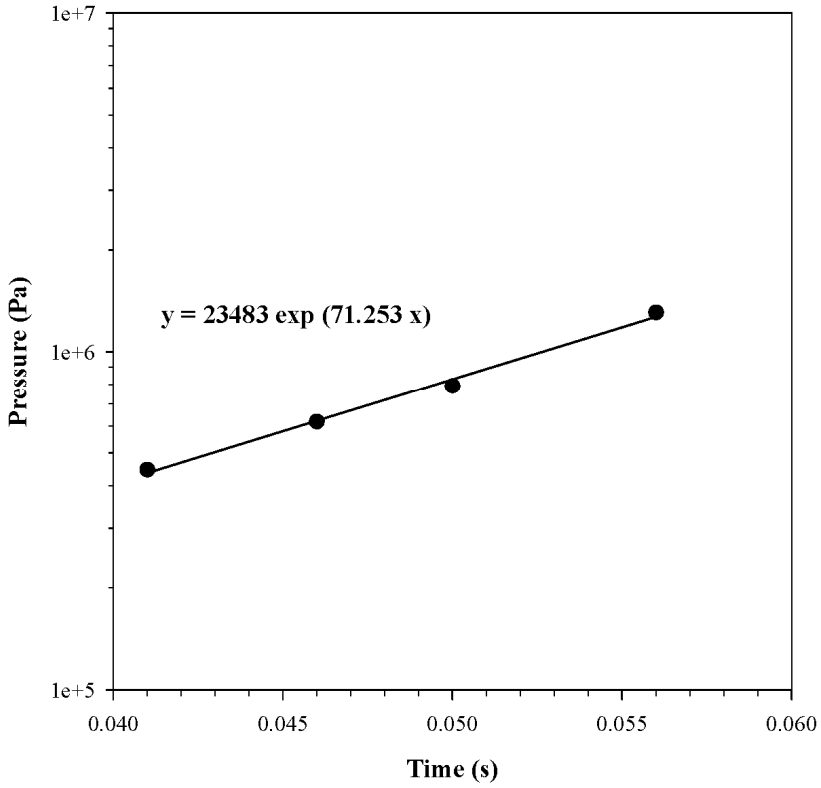

Fig. 3. Comparison of Henry and Fauske choked flow data with homogeneous flow prediction, stagnation pressure = 1.48E6 Pa (200 psig)

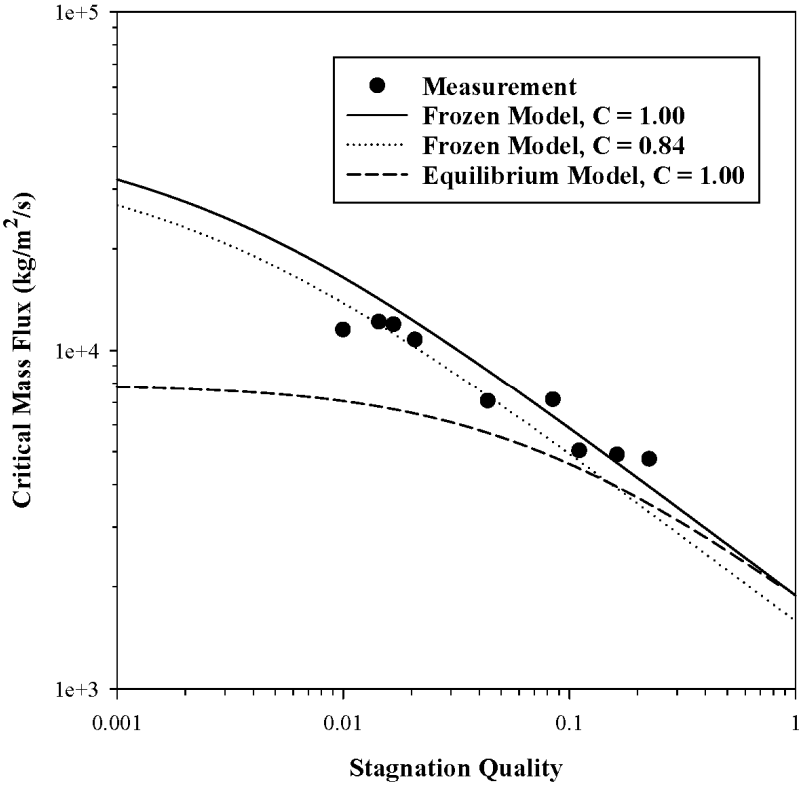

Fig. 4. Comparison of Henry and Fauske choked flow data with homogeneous flow prediction, stagnation pressure = 2.17E6 Pa (300 psig)

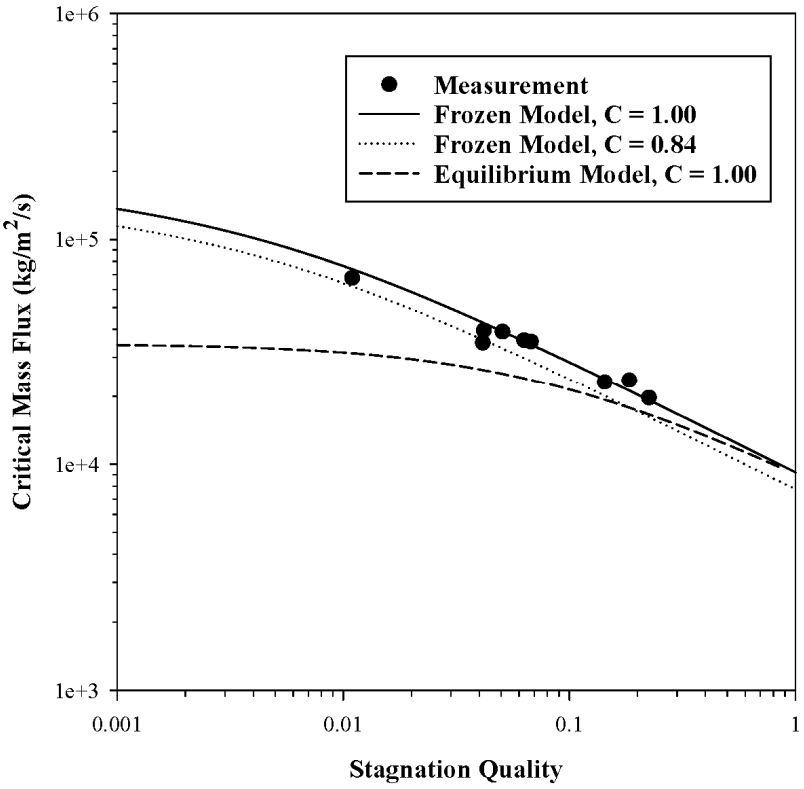

Fig. 5. Correlation of pressure transients for resin vent tests 14 and 15 after disk rupture

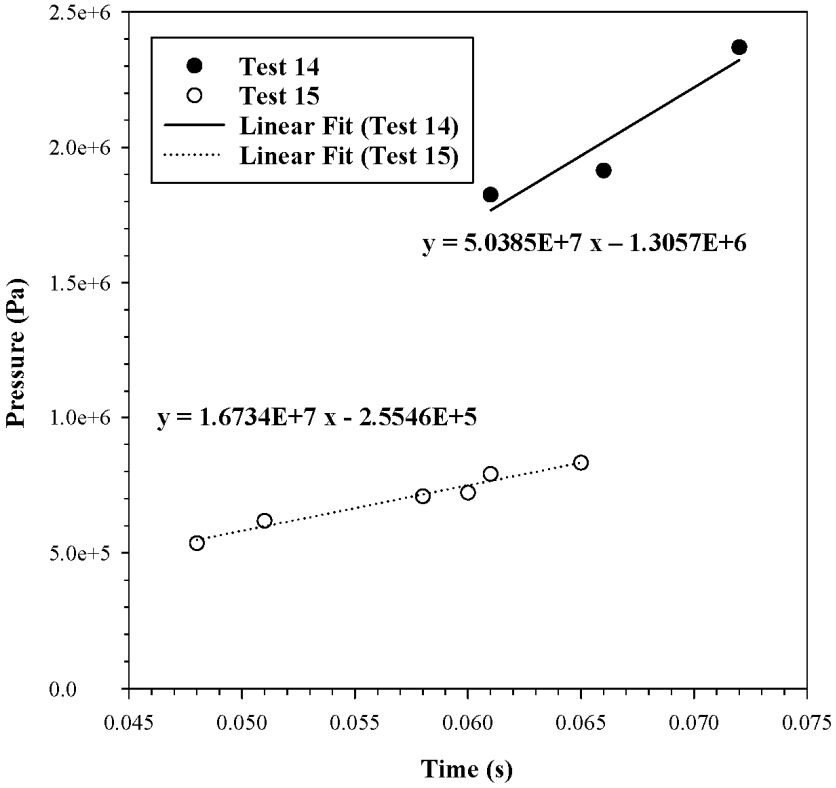

Fig. 6. Comparison of measured and predicted pressure transients for resin vent tests 14 and 15, without runaway reaction effect

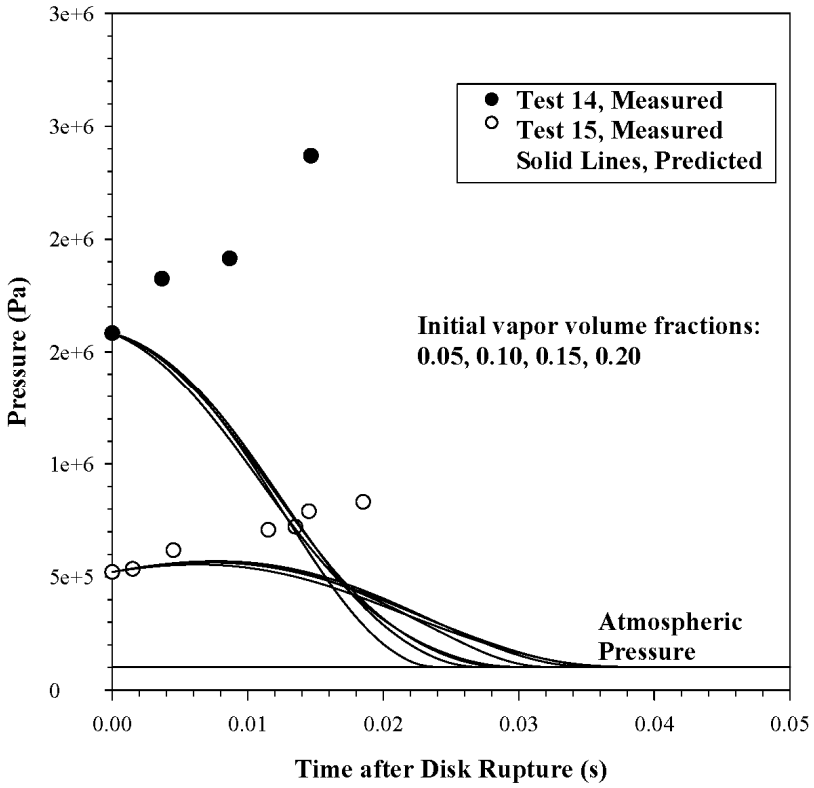

Fig. 7. Comparison of measured and predicted pressure transient for resin vent tests 14 and 15, with runaway reaction effect